

# We are IntechOpen, the world's leading publisher of Open Access books Built by scientists, for scientists

6,900

Open access books available

186,000

International authors and editors

200M

Downloads

Our authors are among the

154

Countries delivered to

TOP 1%

most cited scientists

12.2%

Contributors from top 500 universities



WEB OF SCIENCE™

Selection of our books indexed in the Book Citation Index  
in Web of Science™ Core Collection (BKCI)

Interested in publishing with us?  
Contact [book.department@intechopen.com](mailto:book.department@intechopen.com)

Numbers displayed above are based on latest data collected.  
For more information visit [www.intechopen.com](http://www.intechopen.com)



# **An overview of radio over fibre systems for 60-GHz wireless local area networks and alternative solutions based on polymer multimode fibres**

Christophe Loyez, Christophe Lethien,  
Jean-Pierre Vilcot and Nathalie Rolland

*Institut d'Electronique, de Microélectronique et de Nanotechnologie, UMR CNRS 8520  
Villeneuve d'Ascq, FRANCE*

## **1. Introduction**

This chapter deals with innovative optical systems specific to the high-data-rate hybrid networks operating in the millimetre-wave frequency band. With the incoming of high-data-rate communications protocols, the Radio Frequency (RF) systems operating in the near 60-GHz frequency band are a current alternative to the conventional Ultra Wide Band (UWB) technologies which are limited by drastic power regulations (-41dBm/MHz). To enhance the connectivity of the 60-GHz Wireless LANs, a vast amount of Radio over Fibre (RoF) systems have been developed by the international research community and their performances are demonstrated for data rate in the range of several hundredths of Mbps. Most of them are based on Single Mode Fibres (SMF) assuming that an obvious optical transmission of the 60-GHz carrier signal is required: this chapter will detail the main principles of usual SMF RoF systems. In particular, such systems have to meet specific requirements concerning the access points to prevent degradation performance due to limitations such as the chromatic dispersion inherent to the optical fibre and owing to the phase-noise of the 60-GHz signal. We conclude the compliance of the SMF RoF systems with low-cost applications is still difficult due to the sensitivity of SMF regarding to a misalignment between the fibre core and the active area of the electro-optic and optoelectronic converters. The weak tolerance regarding to an offset launch increases the connection cost. To get rid of the limitations described above, we propose alternative solutions to SMF techniques assuming that the optical transmission of the 60-GHz carrier signal is not necessary required. These solutions for hybrid optical-wireless networks are based on Polymer MultiMode Fibres (PMMF) and include novel monolithically integrated 60-GHz RF systems. The following topics will be detailed in this chapter:

- the usual topologies and requirements of 60-GHz SMF RoF systems.
- a first alternative based on a subcarrier radio signal transmission over PMMF for 60-GHz WLAN using a phase-noise cancellation technique

-a second one involving an impulse system for 60-GHz wireless networks based on PMMF.

## 2. 60-GHz RoF system based on Single Mode Fibres

### 2.1 Topologies of 60 GHz SMF RoF systems

The most popular topologies of 60-GHz RoF systems are still today based on SMF solutions. The aim of such architectures is to transmit efficiently a millimetre-wave signal over a few dozen of kilometres. This objective is motivated by the fact the 60 GHz frequency sources have to meet strong requirements of phase-noise and frequency stability which are not compliant with a real integration of the access points. The characteristics of these SMF systems are described by the figure 1. The millimetre-wave signal cannot directly modulate the bias current of usual lasers having limited modulation bandwidth. By the way, an external modulation is achieved in most of the SMF topologies involving Optical External Modulators (OEM) such as an Electro-Absorption Modulator or an interferometric Mach-Zehnder Modulator (Vegas Olmos 2008). The modulated optical signal suffers from the chromatic dispersion which induces severe link budget penalties even if the photodetector (PD) owns a sufficient detection bandwidth. Several techniques have been investigated to overcome this limitation. We can note the chromatic dispersion compensation and the achievement of single Sideband optical sources (Woo-Kyung Kim 2008). To relax the constraints of frequency bandwidth, solutions performing the optical transmission of sub-harmonic Local Oscillator signals on SMF have been developed. Good performances are obtained for most of these SMF solutions which are well suited for inter-building optical transmission.

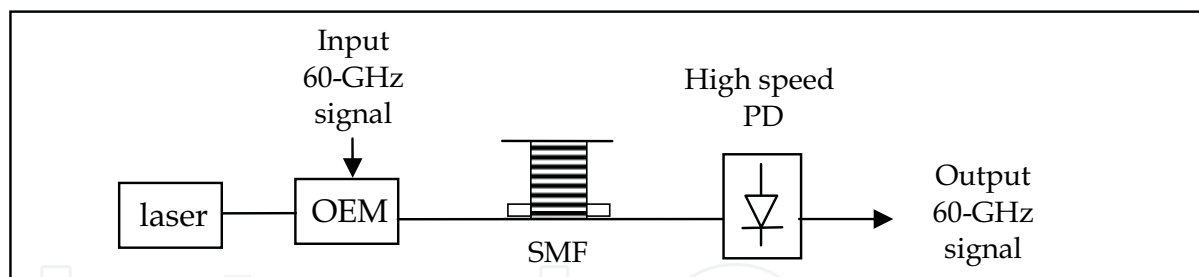


Fig. 1. 60-GHz RoF SMF system

### 2.2 Evolution towards PMMF systems

For short distances in the range of a few hundredth of meters, alternative solutions based on PMMF optical solutions can be used especially for in-building communication. Polymer fibre has been chosen since its easy handling and connection is a real asset compared to the silica fibre: clip-on connector has been developed as to be fixed directly on the external coating of the polymer fibre without the use of expensive tools like in the silica fibre world. Even if these polymer optical fibres exhibit some drawbacks – main one is its high attenuation –, they are well matched to a small office/home office environment use and open the road of the “do it yourself” concept. The chapter titled “Potentialities of multimode fibres as transmission support for multiservice applications: from the wired

small office/home office network to the hybrid radio over fibre concept” summarizes the properties of such a fibre.

The techniques describe hereafter overcome the phase-noise limitation and enable the use of fully integrated oscillator in access points, such as MMIC (Monolithic Microwave Integrated Circuit) oscillators which exhibits a die size less than  $1\text{mm}^2$ . Then, the optical transmission of the 60-GHz local oscillator is not the most interesting solution since fibre-radio systems based on a simple RF architecture using optical COTS (commercial off the shelf) components can be efficient.

### 3. Self-heterodyne system

#### 3.1 Overall description

This first topology includes a self-heterodyne device based on the RF transmission of an additional signal carrier. This topology is depicted by the figure 2: a Vector Signal Generator generates the desired data signal (modulation scheme, data rate) on a 500 MHz subcarrier signal. 500 MHz is chosen to be compatible with the Vector Signal Analyser (VSA) performance, even though a PMMF (62.5  $\mu\text{m}$  core diameter) could transmit microwave signal at higher frequencies due to its high optical bandwidth. Before the optical transmission, Transmitter / Receiver (T/R) modules performs the 60-GHz radio transmission of the resulting subcarrier signal. These modules described hereafter include a phase-noise cancellation technique. At the output of the receiver, this recovered IF signal directly modulates the current of a 850 nm distributed feedback laser. The optical signal is transmitted through the PMMF before to be collected by a multimode pigtailed photodiode. Then, a vector signal analyser measures the rms EVM of the recovered signal. The used PMMF is a perfluorinated graded index polymer optical fibre (PF GIPOF). This one has a 100 m length and owns a bandwidth-length product close to  $600\text{MHz.km}$

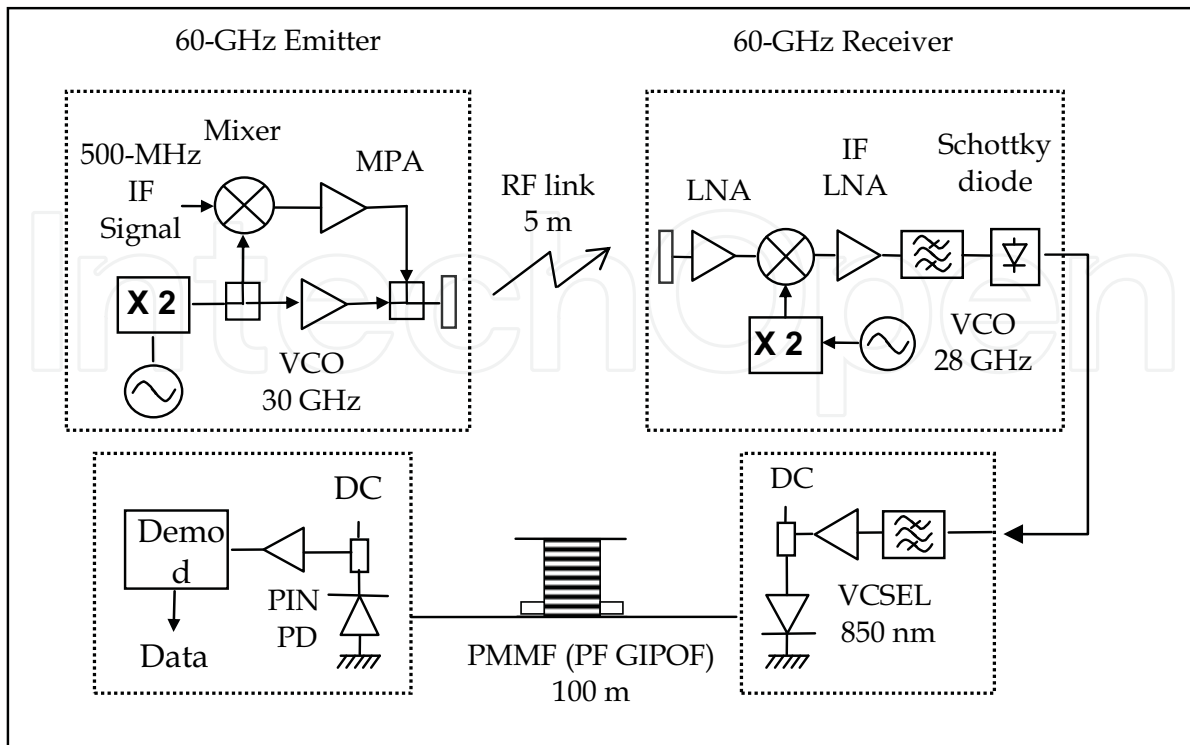


Fig. 2. Self-heterodyne / IF over MMF system

### 3.2 60GHz T/R modules including the phase-noise cancellation technique

In order to cancel the phase-noise, two RF signals with correlated phases are transmitted in order to perform a frequency mixing between them in the receiver. Exploiting the large amount of spectral resources of the 60 GHz band, this kind of solution has already been reported (Shoji 2002). Nevertheless, such systems had, up to now, the drawback of degrading the Carrier-to-Noise power Ratio of the recovered signal. In comparison with a conventional system including LOs with excellent phase-noise, this degradation is at least of 9 dB. The architecture of our system cancels the phase-noise without significant degradation of the CNR. This system is lightly different from a conventional heterodyne system, especially for the transmitter which is designed to transmit an additional signal  $S_c(t)$ . Nevertheless, this architecture is still convenient since it takes advantage of the naturally strong power of the LO pump signal. Figure 2 describes in details the transceiver topology. Before the up-conversion of the IF signal  $S_{IF}(t) = A_0 \cos(2\pi \cdot f_{IF}t + \phi_{IF}(t))$  with  $f_{IF} = 500$  MHz, the LO signal is separated in two paths. The first path provides a pump signal to up-convert the IF signal as in a conventional heterodyne transmitter. The second path delivers the LO signal which is amplified before emission. By this way, we control the power of each signal and we prevent the power amplifier from compression due to the additional signal. The global emitted signal is then expressed as follows:

$$S(t) = S_C(t) + S_{RF}(t) = A \cos(\omega_c t + \phi_c(t)) + A \cos((\omega_c + \omega_{RF})t + \phi_{RF}(t)) \quad (1)$$

with :

$$f_c = \frac{\omega_c}{2\pi} = 60 \text{ GHz and } f_{RF} = \frac{\omega_{RF}}{2\pi} = f_c + f_{IF} = 59.5 \text{ GHz}$$

Assuming that the phase-noise is much lower for the IF signal than for the LO, the correlation between the signals is verified. The signal propagation is performed with directive antennas. The receiver presents a conventional topology. After propagation, the two transmitted signals are down-converted by using a LO whose phase-noise can be very detrimental. During these operations, the phase-noise of the two resulting signals  $S'_C(t)$  and  $S'_{RF}(t)$  increases but the phase correlation between them is not affected. The global signal  $S'(t)$  is then described by the expression (2) :

$$S'(t) = S'_C(t) + S'_{RF}(t) = A' \cos((\omega_c - \omega_{LO})t + \phi'_c(t)) + A' \cos((\omega_c + \omega_{IF} - \omega_{LO})t + \phi'_{RF}(t))$$

$\phi'_c(t)$  : Cumulated phase-noise contributions of T/R local oscillators.

$$\phi'_{RF}(t) = \phi'_c(t) + \phi_{FI}(t) + \phi_0 ; f_{OL} = \frac{\omega_{OL}}{2\pi} = 56 \text{ GHz} \tag{2}$$

Then, an IF mixer based on a polarized Schottky diode performs a frequency mixing between the two input signals  $S'_C(t)$  and  $S'_{RF}(t)$ . After a low-pass filtering, the recovered IF signal  $m(t)$  is then expressed by the equation (3) :

$$m(t) = S'(t)^2 * h_{IF}(t) = A'^2 \cos(\omega_{IF}t + \phi_{IF}(t) + \phi_0) \tag{3}$$

This brief theoretical analysis shows that the Schottky diode mixer acts well as a cancellation device of phase-noise by recovering the original signal without contributions of the T/R LOs. To verify experimentally the cancellation of phase-noise, the T/R modules described above have been achieved by using a MMIC technology. In a first place, the T/R LOs were replaced by synthesized signal generators. Figure 3 presents characteristics of the input signal. The signals  $S'_C(t)$  and  $S'_{RF}(t)$  cumulate the phase-noise of T/R LOs as shown figures 4 and 5. We can note the strong similarity between the two spectral densities due to the phase correlation. The input signal levels are adjusted to ensure an equal power emission  $P_T$  equal to 5 dBm for both the signal  $S_{RF}(t)$  and  $S_C(t)$ . The cumulate gain of the T/R antennas,  $G_T(\text{dB})$  and  $G_R(\text{dB})$ , is around 16 dB. Up to the input of the Schottky diode, the power equality of the  $S'_C(t)$  and  $S'_{RF}(t)$  signals is preserved using a broadband IF LNA. After the Schottky diode mixer, the phase-noise of the resulting signal  $m(t)$  drops drastically as illustrated the figure 6, which shows that the cancellation of local oscillator phase-noise has been performed successfully. The only difference between the input and output signals is due to the thermal noise  $\text{Geq.Feq.k.To} = -112 \text{ dBc/Hz}$  in this case.

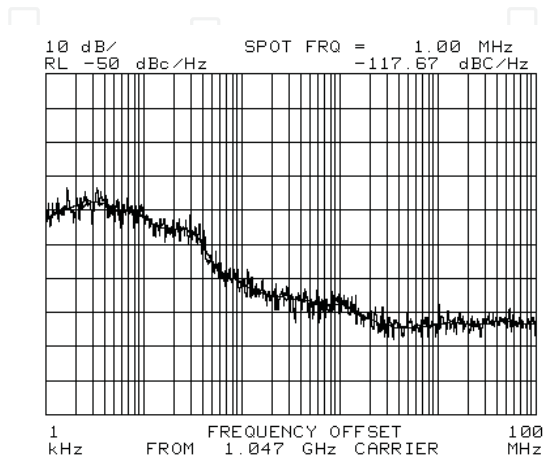


Fig. 3. Phase noise of the Input IF signal

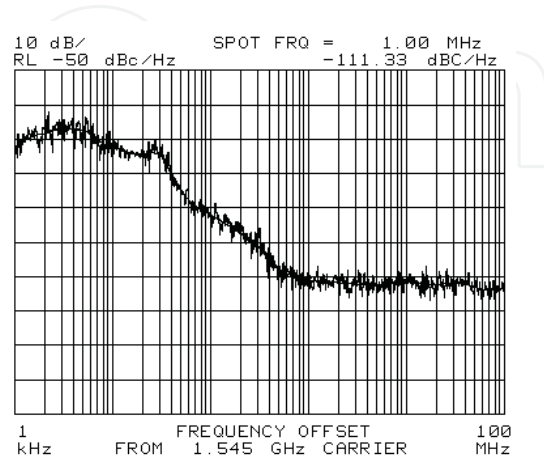
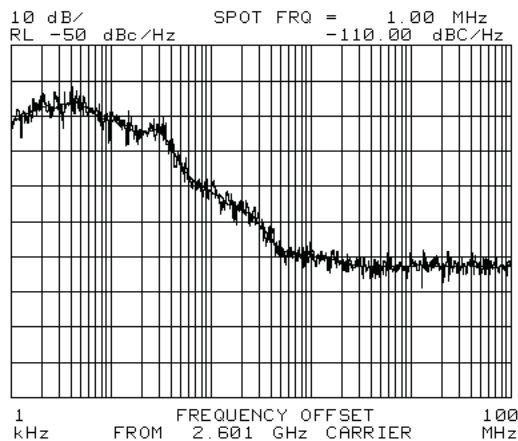
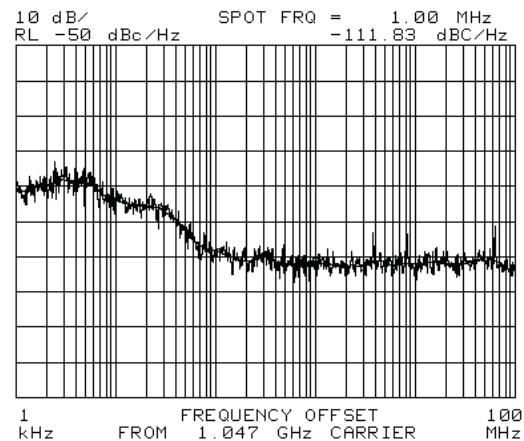


Fig. 4. Phase noise of the signal  $S_c'(t)$



Fig. 5. Phase noise of the signal  $SRF'(t)$ Fig. 6. Phase noise of the output signal  $m(t)$ 

As announced by the equation (3), the residual phase-noise is only the fact of the properties of the signal  $S_{IF}(t)$  and drops below -90 dBc/Hz at 10 kHz off-carrier. Such performances are very attractive in millimeter band. Secondly, MMIC VCOs associated to a frequency multiplication module were used as T/R LOs.

Even if these characteristics of phase-noise are very mitigated by additional parasitic signals, the phase-noise of the output signal  $m(t)$  is still rigorously unchanged. This result shows that MMIC VCOs with degraded characteristics of phase-noise can be included as LO in T/R modules by using this approach.

### 3.3 Noise Figure considerations and Carrier to Noise Ratio Measurements

The comparison of phase-noise between the  $SRF'(t)$  and  $m(t)$  signals, respectively plotted in figures 5 and 6, shows a strongly similar contribution of the thermal noise equal to -112 dBc/Hz. This means that the CNR level remains unchanged before and after the cancellation device. In this part, we deal with the conversion losses  $L_d$  of the Schottky diode mixer and its impact on the noise figure  $F_{eq}$  of the receiver. In particular, we detail the appropriate design to prevent noise figure and, by the way, CNR degradations. As described by the Friis formula (4), the power gain and noise figure of each component are needed to determine  $F_{eq}$ .

$$F_{eq} = F_{LNA} + \frac{(F_{MIX} - 1)}{G_{LNA}} + \frac{(F_{LNA\_IF} - 1)}{G_{LNA} \cdot G_{MIX}} + \frac{(F_{det} - 1)}{G_{LNA} \cdot G_{MIX} \cdot G_{LNA\_IF}} + \frac{(F_{MPA\_IF} - 1)}{G_{LNA} \cdot G_{MIX} \cdot G_{LNA\_IF} \cdot G_d} \quad (4)$$

$$P_{IN} = P_T \cdot G_T \cdot G_R \cdot \left( \frac{\lambda}{4\pi \cdot R^2} \right) \cdot G_{LNA} \cdot G_{MIX} \cdot G_{LNA\_IF} \quad (5)$$

These data are summarized in Table 1. The RF LNA and mixer are designed to reduce the noise figure  $F_{eq}$ . For a conventional receiver, the value  $F_{eq}$  would be around 6 dB. In the case of this system, the conversion losses  $L_d$  have to be measured.

Component	LNA	Mixer	LNA_IF	Diode Mixer	MPA_IF
Gain (dB)	40	-12	GLNA_IF	Gd = - Ld	20
Noise Factor (dB)	6	15	3	Fd	3

Table 2. Gain and noise figure of components in the receiver

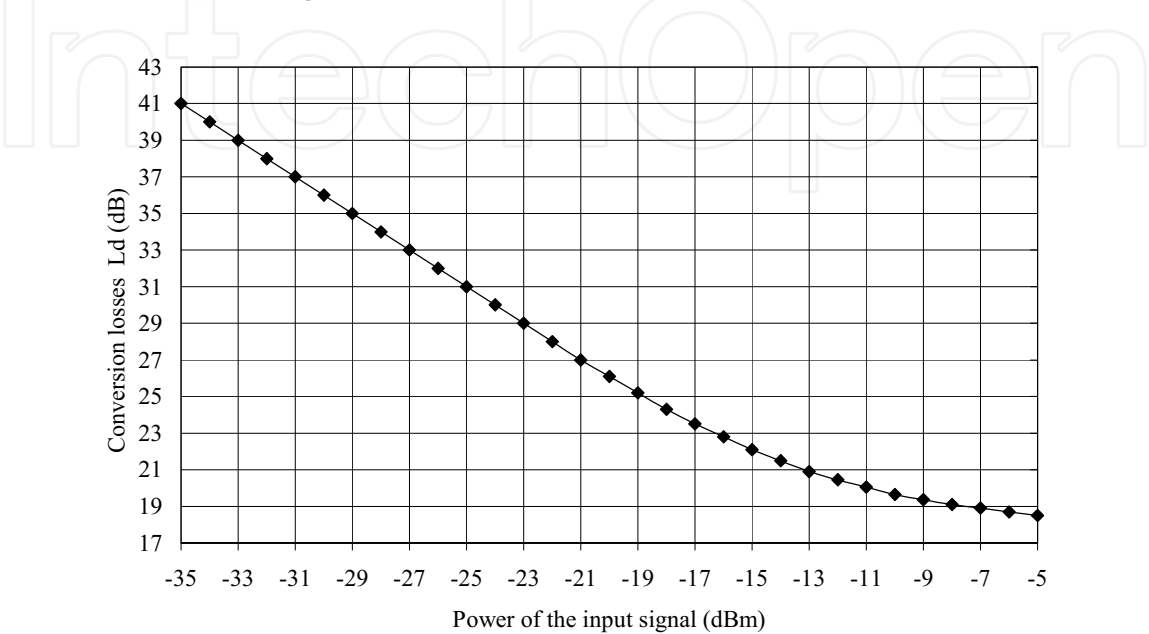


Fig. 7. Conversion losses  $L_d$  of Schottky diode mixer

The Schottky diode mixer presents important conversion losses, especially for a low input power. Figure 7 displays these conversion losses,  $L_d$ , versus the input signal power  $P_{in}$ . The link budget, expressed by equation (5) and applied to these experimental results, concludes that the conversion losses  $L_d$  could reach up to 40 dB for a propagation distance of 15 meters. As a consequence, such conversion losses had to be taken into account in the receiver design concerning the noise figure.

According to the results described above, the Friis formula (4) and the link budget (5) enable to calculate the degradation of the noise figure  $F_{eq}$  versus the propagation distance. Concerning the noise figure  $F_d$  of the Schottky diode mixer, we assumed  $F_d = L_d + 9$  dB when the power equality of the two input signals,  $S_C'(t)$  and  $S_{RF}(t)$ , is ensured. In these conditions, a gain of LNA equal to 15 dB allows a transmission distance of 15 meters with a  $F_{eq}$  degradation less than 1 dB.

This approach of the receiver design prevents theoretically the noise figure from an additional damage due to the cancellation. To confirm these results experimentally, measurements of the CNR, versus the propagation distance, have been achieved respectively for the  $S_{RF}'(t)$  and  $m(t)$  signals. For these measurements, we integrated the approximate spectral power noise density in considering an equivalent noise bandwidth of 25 MHz. In figure 8, these experimental results confirm that the CNR of the received signal undergoes no significant degradation due to the phase-noise cancellation.



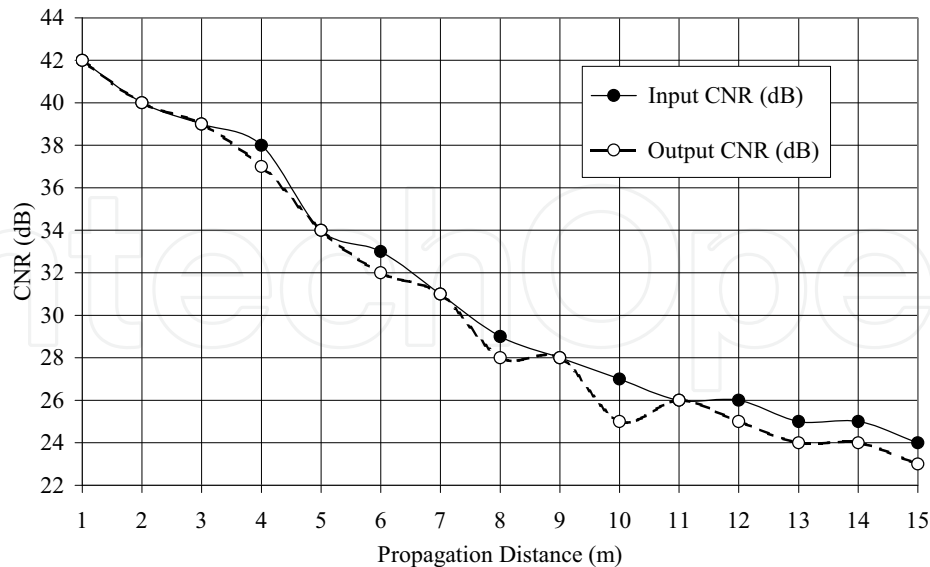


Fig. 8. CNR Measurements

### 3.4 EVM measurements

The 500 MHz modulated subcarrier is generated by a vector signal generator. The modulation schemes are QPSK, 16QAM and 64QAM allowing data-rates up to 300 Mbps. The T/R base-band filters are root raised-cosine filters with a roll-off factor  $\alpha = 0.35$ . The recovered signal is analysed by using a vector signal analyser. Experimental results of rms EVM for different modulation schemes are promising. We can note that these results are not strongly limited by the optical link. The EVM measurements have been performed as a function of the RF range. The results corresponding to RF range equal to 5 meters are presented hereafter: EVM results are less than 6.5% value for a QPSK 100 Mbps transmission. Since a direct QPSK 100 Mbps link between the ESG and the VSA leads to EVM results in the range of 4% to 5%, the degradation of the signal quality due to the overall transmission is not significant. Reaching such results using only MMIC VCOs is unrealisable without phase-noise cancellation technique. To transmit higher data rate, 16QAM modulation is tested up to 200 Mbps. For this case, EVM results never exceed 6.5 % even though measurement of a direct link provides EVM in range of 3.5%. The constellation diagram of figure 9 shows that this weak degradation is only due to thermal noise and non-linear behaviour of the 60-GHz transceiver. No alteration due to phase-noise can be observed, verifying the performance of phase-noise cancellation technique. To reach data rates of 300 Mbps, 64QAM modulation scheme is used. Once again, the phase-noise cancellation is applied and thermal noise and non-linearities are the only degradation factors. EVM results are in the range of 6 %: they are very promising and can be greatly enhanced by using a RF system having a better 1dB compression point. It will be then possible to transmit RF signals with the same power level (5dBm) but with a more important back-off.

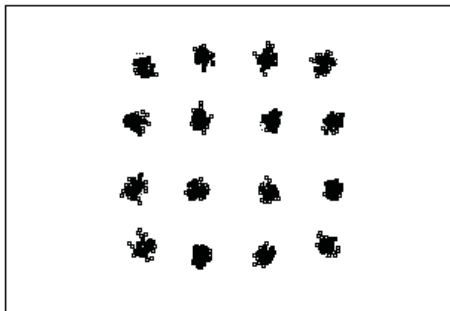


Fig. 9. Constellation Diagram (16QAM - 200 Mbps)

3.5 Multiple access strategy

A weak spectral efficiency is the only drawback of the topology detailed above. Furthermore, the multiple access strategy of such a technique is reduced to Frequency Division Multiple Access (FDMA). To reduce the spectral bandwidth of a channel, it is worth transmitting the additional carrier with a frequency  $f_c$  very close to one limit of the RF signal spectrum. Further works are in progress to achieve high-data-rate FDMA systems having an excellent trade-off between channel capacity and architecture compactness.

4. 60-GHZ Frequency Up-Converted Impulse System

4.1 Physical and MAC layers considerations

Concerning the physical layer, the main characteristic of this 60-GHz system is to inhibit the impact of both the LO phase-noise and the system non-linearities on signal quality. By the way, the Pulse Position Modulation (PPM) technique applied to sub-nanosecond pulses that are up-converted in the 60-GHz band is an attractive solution: the data information supported by the pulse position can not be affected by any phase deviation or power saturation. Furthermore, the use of sub-nanosecond pulses performs a wide spread spectrum which robustness against signal fading due to multi-path propagation has already been widely reported. Another consideration is relative to the Medium Access Control (MAC) layer: contention-based protocols such as CSMA/CA (Carrier Sense Multiple Access with Collision Avoidance) present suitable abilities for ad hoc network performance (Sobrinho 1999). To multiplex the radio-communications, we use such protocols based on a Time Hopping (TH) technique which takes advantage of the characteristics of the UWB pulses (Bo Hu 2005). Figure 9 illustrates the PPM and TH operations for a specific time interval.

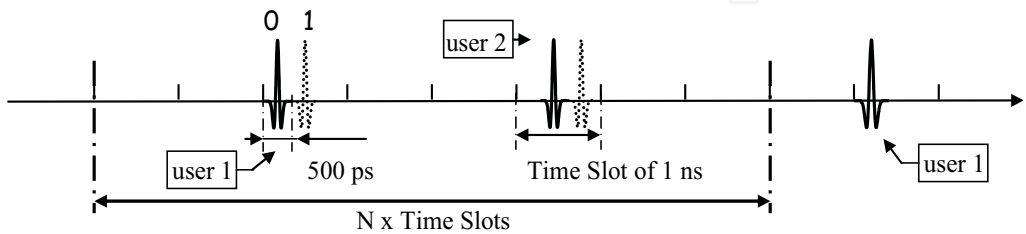


Fig. 10. PPM and TH technique using sub-ns pulses

4.2 Overall topology

The overall topology is depicted in the figure 10. The RF emitter and receiver include MMICs realized with different pHEMTs from OMMIC foundry (ft up to 120 GHz). The main component of the emitter is a pulse generator. This generator consists of a high-speed NOR logic gate associated to a varactor diode which enables to delay the relative position of generated pulses. The 60-GHz carrier signal is generated by a 30-GHz VCO associated to a frequency doubler. The frequency up-conversion of the sub-nanosecond pulses is obtained by modulating the amplitude of the 60-GHz OL signal. This Amplitude Modulation (AM) is performed by a switch having a SPDT (Single-Pole Double-Throw) topology and ensuring an isolation of more than 23 dB. The RF modulated signal is then amplified using a Medium Power Amplifier (MPA) which provides an output power of 16 dBm. The receiver includes a low noise amplifier, a RF detector and a correlator. The Low-Noise Amplifier has a Noise Figure equal to 6.5 dB and a power gain of 42 dB at 60-GHz. The RF detector performs the envelope detection of 60-GHz up-converted IR-UWB pulses. Next, the correlator mainly consists of a matched filter and a fast sampling and hold amplifier (SHA). Another pulses generator is used to trig this SHA. This second pulses generator is synchronised with the incoming signal by using a specific synchronisation technique which renders output binary data (Deparis 2006).

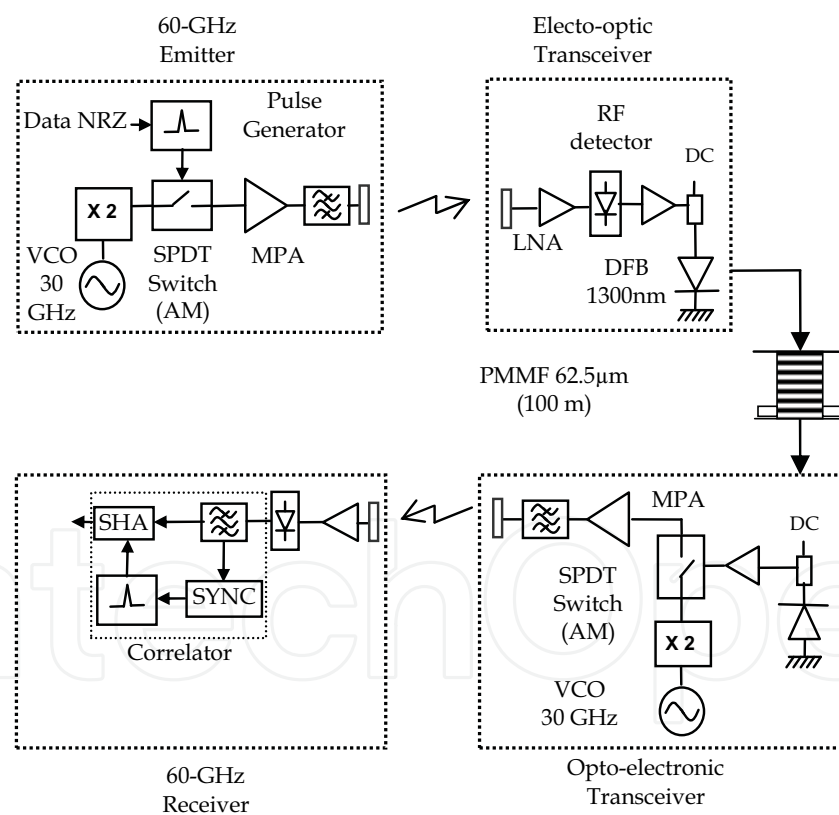


Fig. 11. multi-hops opto-RF transmission

### 4.3 Experimental Set-Up and Results

The multi-hop transmission is described in Figure 10: the binary data stream is provided by a data timing generator Tektronix. These data modulate the pulse position of a first transmitter operating at 60 GHz. After the MPA, the time evolution of the RF signal is measured and shows an isolation between the ON-state and the OFF-state greater than 20 dB. The pulse width is close to 300 ps and corresponds to a good trade-off between channel capacity and spectral band filling: the narrowness of the pulse width enables to decrease the probability of collisions between users and offers a sufficient spread spectrum to prevent signal fading due to multipath propagation. The radiated signal has a peak power of 22 dBm and is transmitted over a range of 4 meters. The emitter and receiver antennas have a 3dB aperture beam-width equal to 60 degrees. The RF part of the electro-optic transceiver is only composed by a LNA and a detector enabling to recover the pulse envelope. Then, these pulses modulate the intensity of a Distributed Feedback Laser (DFB) operating at 1300nm. The intensity modulated optical signal is transmitted through a PMMF based on perfluorinated polymer and having a core diameter close to 62.5  $\mu\text{m}$ . The measured optical power after 100 m link length is -4dBm (optical).

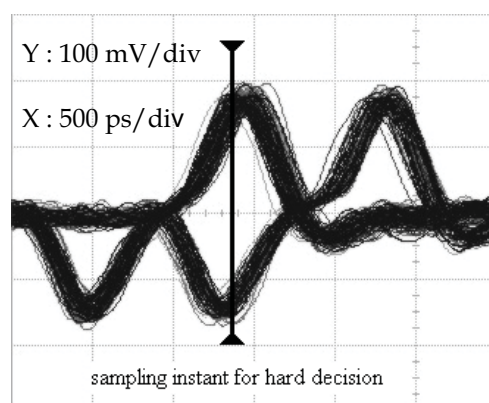


Fig. 12. Eye diagram of received PPM signal

A low cost PIN photodiode followed by a DC-6GHz amplifier delivers the sub-nanosecond pulses to the RF part of the optoelectronic transceiver. Recovered pulses modulate a second 60-GHz LO signal. The modulated signal is amplified in the same manner as for the first hop. Once again, the modulated RF signal is transmitted over a distance of 4 meters. Same antennas as for the first RF hop are used. The MMW receiver, as the first one, is only composed by a LNA and a detector which enables to recover the pulse envelope. At this stage, the eye diagram of the received pulse stream can be observed in Figure 11. The eye aperture shows the high quality of the multi-hop transmission. These results are quantified by BER measurements on a logic analysis system: for a data rate of 100 Mbps, BER measurements reach values greater than  $10^{-6}$  and validate by this way the MMW RoF system performance. Further experimental results have been led successfully for data rates up to 200 Mbps with BER measurements under the threshold value of  $10^{-6}$  without using additional signal processing.

## 5. Conclusion

In this chapter, we have presented two innovative hybrid systems based on specific 60-GHz wireless systems. The compliance of these systems with opto-RF transceivers has been experimentally demonstrated, proposing by the way two efficient alternatives to 60-GHz SMF RoF systems. Lower cost optical solutions, i.e. 62.5µm core polymer fibre and IM-DD technique, were used.

We have detailed an unidirectional transmission by using a PMMF based optical link operating at 1300nm. Assuming the low material dispersion properties (and so the potential high bandwidth) of the PMMF in a wide wavelength range (from 800nm to 1400nm), the bidirectional transmission could be performed by using the Wavelength Division Multiplexing (WDM) technique available for the Glass Multimode Fibre.

## 6. References

- Bo Hu; Beaulieu, N.C ; *Accurate performance evaluation of time-hopping and direct-sequence UWB systems in multi-user interference*, IEEE Transactions on Communications, Volume 53, Issue 6, June 2005 Page(s):1053 – 1062
- Deparis, N.; Boe, A.; Loyez, C.; Rolland, N.; Rolland, P.A.; *Receiver and Synchronization for UWB impulse radio signals*, 2006 IEEE MTT-S - 11-16 June 2006- San Francisco, California
- Shoji, Y.; Hamaguchi, K.; Ogawa, H.; *Millimeter-wave remote self-heterodyne system for extremely stable and low-cost broad-band signal transmission*, IEEE Transactions on Microwave Theory and Techniques, Volume 50, Issue 6, June 2002 Page(s):1458 - 1468
- Sobrinho, J.L.; Krishnakumar, A.S.; *Quality-of-service in ad hoc carrier sense multiple access wireless networks*, IEEE Journal on Selected Areas in Communications, Volume 17, Issue 8, Aug. 1999 Page(s):1353 - 1368
- Vegas Olmos, J.J.; Kuri, T.; Sono, T.; Tamura, K.; Toda, H.; Kitayama, K.-i.; *Reconfigurable 2.5-Gb/s Baseband and 60-GHz (155-Mb/s) Millimeter-Waveband Radio-Over-Fiber (Interleaving) Access Network*, Journal of Lightwave Technology, Volume 26, Issue 15, Aug.1, 2008 Page(s):2506 - 2512
- Woo-Kyung, Kim; Woo-Jin Jeong; Soon-Woo Kwon; Myoung-Keun Song; Geun-Sik Son; Woo-Seok Yang; Hyung-Man Lee; Han-Young Lee; *60 GHz Optical Carrier Generation Using a Domain Reversed LiNbO<sub>3</sub> Optical Modulator*, Journal of Lightwave Technology, Volume 26, Issue 14, July15, 2008 Page(s):2269 - 2273



## **Optical Fiber New Developments**

Edited by Christophe Lethien

ISBN 978-953-7619-50-3

Hard cover, 586 pages

**Publisher** InTech

**Published online** 01, December, 2009

**Published in print edition** December, 2009

The optical fibre technology is one of the hot topics developed in the beginning of the 21st century and could substantially benefit applications dealing with lighting, sensing and communication systems. Many improvements have been made in the past years to reduce the fibre attenuation and to improve the fibre performance. Nowadays, new applications have been developed over the scientific community and this book fits this paradigm. It summarizes the current status of know-how in optical fibre applications and represents a further source of information dealing with two main topics: the development of fibre optics sensors, and the application of optical fibre for telecommunication systems.

### **How to reference**

In order to correctly reference this scholarly work, feel free to copy and paste the following:

Christophe Loyez, Christophe Lethien, Jean-Pierre Vilcot and Nathalie Rolland (2009). An Overview of Radio over Fibre Systems for 60-GHz Wireless Local Area Networks and Alternative Solutions Based on Polymer Multimode Fibres, *Optical Fiber New Developments*, Christophe Lethien (Ed.), ISBN: 978-953-7619-50-3, InTech, Available from: <http://www.intechopen.com/books/optical-fiber-new-developments/an-overview-of-radio-over-fibre-systems-for-60-ghz-wireless-local-area-networks-and-alternative-solu>

**INTECH**  
open science | open minds

### **InTech Europe**

University Campus STeP Ri  
Slavka Krautzeka 83/A  
51000 Rijeka, Croatia  
Phone: +385 (51) 770 447  
Fax: +385 (51) 686 166  
[www.intechopen.com](http://www.intechopen.com)

### **InTech China**

Unit 405, Office Block, Hotel Equatorial Shanghai  
No.65, Yan An Road (West), Shanghai, 200040, China  
中国上海市延安西路65号上海国际贵都大饭店办公楼405单元  
Phone: +86-21-62489820  
Fax: +86-21-62489821

© 2009 The Author(s). Licensee IntechOpen. This chapter is distributed under the terms of the [Creative Commons Attribution-NonCommercial-ShareAlike-3.0 License](https://creativecommons.org/licenses/by-nc-sa/3.0/), which permits use, distribution and reproduction for non-commercial purposes, provided the original is properly cited and derivative works building on this content are distributed under the same license.

IntechOpen

IntechOpen